Measurements and Characterization of Twisted Radio Wave Multipath for Indoor Wireless Communication and Security System

S. W. Chen[2], C. K. Seow[1], S. Y. Tan[2] and P. B. De Silva[2]
[1]University of Glasgow, United Kingdom
[2]Nanyang Technological University, Singapore

Abstract-This paper presents a novel twisted radio wave based wireless communication system that has the capability to discriminate against strong reflections in indoor multipath environment. The twisted wave transmitter is designed using a uniform circular array, which is capable of transmitting different OAM modes simultaneously and the receiver is designed to match to the transmitted OAM mode. The measurement results obtained from the experiments carried out in different indoor environments and different propagation scenarios show that our proposed twisted radio wave system can provide a stable transmission link even in the presence of existing ZigBee and Wi-Fi signals, which are operating in the same frequency band. A good general agreement between the simulations and measurement results shows the accuracy and applicability of our proposed wireless communication system in such indoor multipath environments.

1. INTRODUCTION

Twisted radio explores the Orbital Angular Momentum (OAM) of an electromagnetic wave [1-3], where each OAM state is defined by two unique properties: intensity singularity and rotational phase front [4-7]. Each unique intensity singularity and corresponding phase front referred to as particular OAM state of a radio wave. The use of OAM of electromagnetic wave has been thoroughly exploited in the optic regime in the past few decades [8]. Yet, it's a relatively a novel topic for the Microwave regime, as the researchers began to explore the applicability of OAM in wireless communication [9]. It is shown that using these OAM states which are orthogonal to each other, several communication channels can be established simultaneously in the same frequency band. This will lead to an opening of a new era of communication.

Meanwhile, the OAM of a radio wave has been deeply investigated in the radar imaging technology. In [10], Liu et al. proposed an optimization method of antenna radiation pattern to enhance the accuracy of radar target detection, in both range and azimuth dimensions. Liu et al. [11] shows that OAM based radar can acquire azimuth information and enhance target detection capabilities. In addition, Tiezhu et al. in [12] provides a mathematical model to demonstrate the beam steering capabilities and shows that OAM based radar can provide higher resolution for imaging. In [13], Mingtuan et al. shows that using Multiple Signal Classification (MUSIC) algorithm, OAM based radar can achieve super resolution capacity compared to conventional radar while OAM based radar can achieve similar performance similar to conventional radar using fewer samples .

One of the significant milestones of the journey of twisted radio wave is the experiment conducted by Tamburini et al. [9], in 2012, which is the first ever documented experiment for transmission and reception of twisted radio wave in microwave regime at frequency of 2.414 GHz, over a distance of 442m, using a modified parabolic antenna and two horizontally placed Yagi-Uda antennas as transmitter and receiver respectively. In [14], Liu et al. used Vector Network Analyzer (VNA) based uniform circular array of radius 15cm (5λ), at

frequency 9.9 GHz (experimental verification in X band for the first time), to generate high quality vortex beams in anechoic chamber at a distance of 12cm (4λ).

In 2014, Yan et.al [15] successfully conducted a twisted radio wave transmission experiment at a distance of 2.5m and at frequency of 28GHz using Spiral Phase Plates (SPP) to generate and receive twisted radio wave. They successfully multiplexed 4 Gbps to 32 Gbps using 4 OAM modes and 2 polarization. The radiation properties and transmission characteristics have also been theoretically analyzed. In [16], Yan et al. used similar experiment set up mentioned in [15], but in the presence of an Aluminum reflector. The results show that their system performance for the wireless communication link degrades severely in the presence of multipath.

The contribution of this work is to propose a novel twisted radio wave based wireless communication system, which is capable of establishing a stable transmission link in indoor multipath environments and offer various new application such as secure localization [17-21]. First theoretical formulation of twisted radio wave transmission using a circular array of antennas will be presented. Then experimental verification of twisted radio wave using a VNA based virtual circular array of dipole antennas is carried out in the anechoic chamber room and made comparison with the simulation results. By observing the phase pattern generated by twisted radio wave, a specific receiver system has been designed which has the capability of enhancing the Line of Sight (LOS) twisted radio wave signal and mitigating multipath components in indoor environments. Encouraged by the simulations and experimental results, a novel real time twisted radio wave transceiver system has been designed using National Instrument (NI) based Vector Signal Transceiver (VST) model PXIe-5644, which could provide real time and reliable wireless communication in indoor multipath environment. The proposed system is also capable of simultaneously transmit multiple OAM modes. The accuracy and applicability of our proposed system in indoor multipath environments has been presented experimentally in comparisons with respective simulations in different indoor environments.

2. THEORY AND FORMULATION

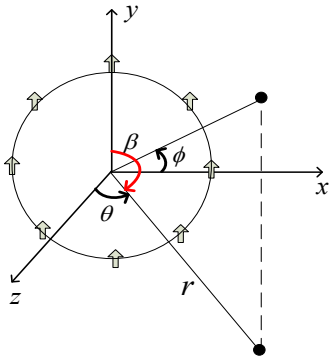

Figure 1: Geometrical arrangement of a circular antenna array of finite length dipole antennas, oriented along y axis.

Fig. 1 shows a uniform circular antenna array which is placed on the *xy* plane with dipole antenna elements oriented along *y* or vertical axis. All the antennas elements are identical and assumed to be omnidirectional. The *N* antenna elements are equidistantly placed along the perimeter of a circle with a consecutive phase difference of $\Delta\phi = 2\pi\ell / N$. ϕ is the azimuth angle and ℓ is the OAM state. The electric field vector $\vec{E}(\vec{r})$ at far field, which consist of *N* dipole antennas of length *L* can be written as [22]

$$\vec{E}(\vec{r}) = \frac{j\eta I_0}{2\pi}\sum_{n=1}^{N}\frac{e^{-jkr_n}}{r_n}e^{j\ell\frac{2\pi(n-1)}{N}}\left[\cos(\frac{kL}{2}\cos\beta_n) - \cos(\frac{kL}{2})\right]/\sin\beta_n\hat{\beta}_n \quad (1)$$

where β_n is the angle measured from the n^{th} element and the direction of E field is along β_n. r_n indicates the distance measured from the n^{th} antenna element. I_0 is the amplitude of the current and k is the wave vector.

3. SIMULATION AND EXPERIMENTAL RESULTS

In order to examine the characteristic of the twisted radio wave, experiments were carried out in an anechoic chamber room with dimension 6m × 3m, as shown in Fig. 2. The dipole antennas of gain 2dBi was used in the experiments. A VNA (Agilent N5244A) based virtual circular antenna array with eight antenna elements is employed to generate the twisted radio wave at f = 2.45 GHz and one receiving antenna is employed to receive the signal. The transmitted power of the system was set to 0.3mW for each antenna element. The radius of the virtual antenna array is 6cm. The receiver plane is 3m away from the antenna array and the measurement window is 20cm × 20cm. The corresponding E field was calculated by substituting $L=\lambda/2$ in the equation (1). Fig. 3 demonstrates the simulation and experimental results for the phase and amplitude distribution of the twisted radio wave. As shown in Fig. 3(a), a change in phase of 360° could be observed when move one circle around the center and the phase difference across the center is 180°. In Fig. 3(b), we can observe that the intensity singularity is at the center of the receiver plane.

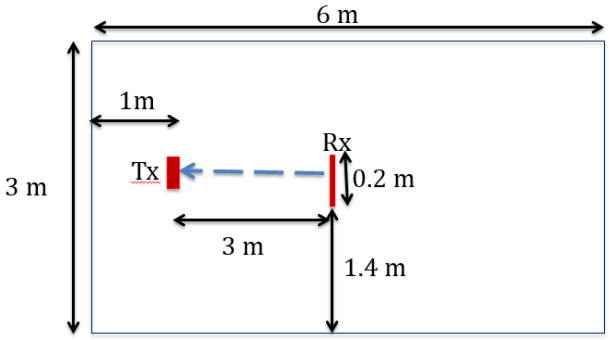

Figure 2: Geometry for the experiments in the anechoic chamber.

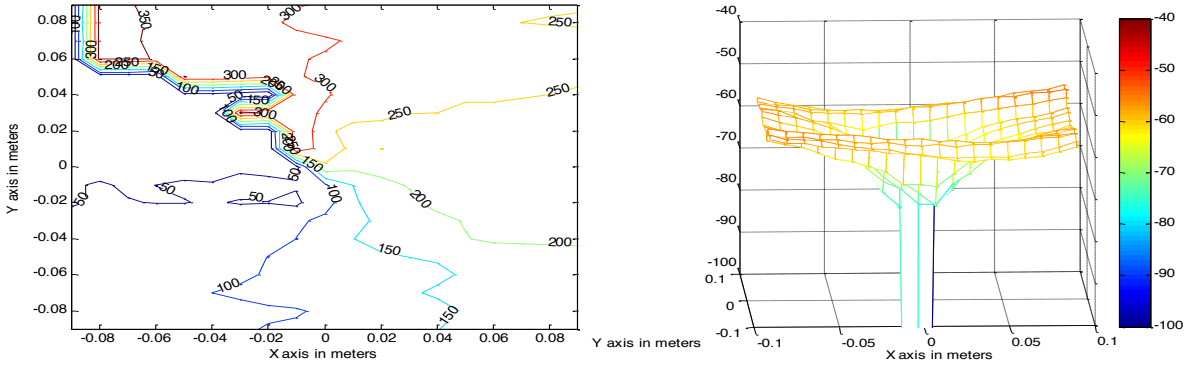

(a) (b)

Figure 3: (a) Experimental result for phase component of the twisted radio wave. (b) Experimental result for the amplitude component of the twisted radio wave.

Fig. 4 depicts the performance of the simulated path loss profile and make comparison with the experimental

result. In the simulation, the measurement range is x from -0.09m to 0.09m with y=0. As shown, the experimental result lies close to the simulated result.

From the experimental result as shown in Fig. 3, it is noted that the phase difference across the center along vertical axis is 180^o and it will reduce when away from the center. Furthermore, in terms of amplitude, no significant difference across the intensity singularity could be observed. By making use of these characteristics, two antennas could be placed along vertical axis with 180^o phase shift is introduced to one of them. This would cause constructive interference of the received signal near the intensity singularity and destructive interference away from it. As a result, this two receiving antenna system will have the ability to enhance the received signal strength of the LOS path and minimize and mitigate the effect of reflections in indoor multipath environments.

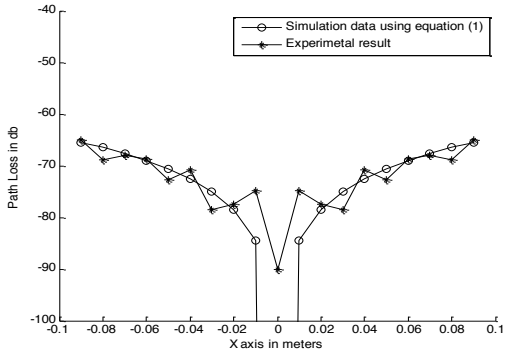

Figure 4: Comparison of path loss profile for simulation and experiment by using one receiving antenna.

In order to evaluate the performance of the two receiving antenna system, first we conducted simulation according to the geometry shown in Fig. 2, but with an addition of an Aluminum reflector placed 2m away from the axis of propagation, which would create a strong reflected signal in addition to the direct LOS signal. In this simulation scenario, we compare the two antenna receiver system with a vertical orientation vs horizontal orientation, where the separation for two antennas under both horizontal and vertical scenario is 18cm. The simulation window size is 20cm along x axis x= -0.1m to 0.1m. Fig. 5(a) shows the corresponding simulation results. It could be observed that two antenna receiver system with vertical orientation shows very stable signal strength while that for horizontal orientation shows large fluctuations up to ±5dB. This results motivates us to design the two antenna receiver with a vertical orientation.

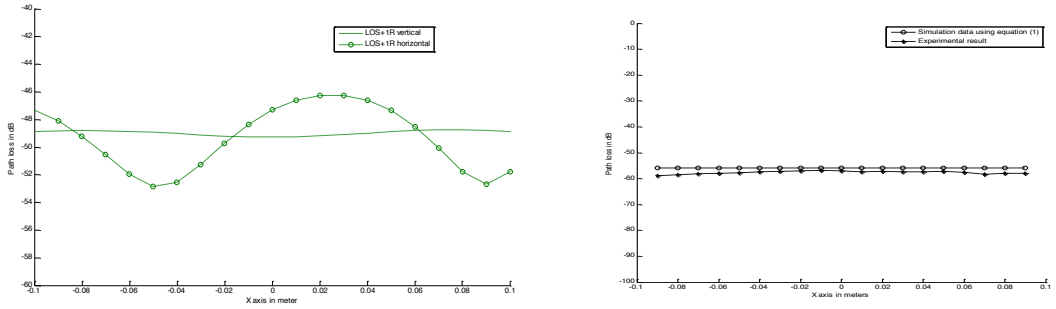

(a) (b)

Figure 5: (a) Comparison of path loss profile for simulation using two receiving antennas placed vertically vs horizontally in the presence of Aluminum reflector placed at 2m away. (b) Comparison of path loss profile for simulation and experiment by using two vertically placed receiving antennas.

To verify the characteristic of the two vertical receiving antenna system, the experiment is carried out in the anechoic room. The measured window size is 18cm. Fig. 5(b) shows the performance of path loss profile by comparing the simulation and experimental result. The experiment results make a good agreement with the respective simulations hence paving the path to design our proposed real time twisted radio wave transceiver system, which is described in the following section.

4. REAL TIME TWISTED RADIO WAVE TRANSCEIVER SYSTEM

The aim of designing this real time twisted radio wave transceiver is to enhance the LOS twisted radio wave signal and mitigate the effect of multipath, which will degrade the performances. The twisted radio wave transmitter is capable of electronically tuning to generate different OAM states as well as to simultaneously transmit multiple channels, modulated with different OAM states, in the same carrier frequency. The receiver system is designed to match to the direct LOS path and discriminate multipath (hereafter referred to as matched receiver). In the following section, simultaneous transmission and reception of 2 channels will illustrated.

The twisted radio wave transmitter, as shown in Fig.6(a), consists of 8 dipole antenna elements (T1 to T8), arranged in a circular array, where the antennas are placed equidistantly on a radius of circle of diameter of 18cm ($\approx 1.5\lambda$). Baseband signal 1 was generated and multiplexed in to 8 different channels before introducing with a progressive phase shift of 45° since it's modulated with OAM mode 1. The phase shifted signals were then up converted with a carrier frequency of 2.45 GHz before going through Low Pass Filter (LPF). The second baseband signal would also be multiplexed to 8 different channels, before being up converted with carrier and going through Low LPF. The modulated baseband signals will be summed up accordingly and transmitted using NI based Vector Signal Transceiver (VST) of model PXIe-5644.

As shown in Fig. 6(b), the matched receiver consists of 2 dipole antennas (R1 and R2) placed across the axis of propagation with a separation of 18cm. The received signals by two antennas will be down converted to the baseband frequency followed by sending through a LPF. Then a relevant phase will be introduced to one of the receiving antenna (depending on the OAM mode of the transmitted signal) in order to extract the baseband signals separately. In order to extract the twisted radio wave signal, which was modulated with OAM 1, 180° Phase shift is required while for that of conventional radio wave signal which is modulated with OAM 0 or conventional radio wave, no phase shift is required. Carrier recovery circuit was used to compensate for frequency and phase difference between the transmitted carrier and the local oscillator carrier at the receiver end. To verify the performance of our system, first we transmitted 1 kHz signal modulated with OAM 1 and 2 kHz signal modulated with OAM 0. At the receiver end, we were able to successfully receive and decode both 1 kHz and 2 kHz signal. A live demonstration of the above system with the capability of transmission and reception of 2 different songs (Chinese song modulated with OAM 1 and English song modulated with OAM 0) in the same frequency was demonstrated to the interested parties of the project.

Next set of experiments were carried out to evaluate the performance of the twisted radio wave transceiver system in indoor multipath environment. In this set of experiments, only one baseband signal (modulated with OAM state 1) was used. The carrier frequency was set to 2.45 GHz. First we observed the background signal strength of Wi-Fi signals using a spectrum analyzer and the recorded values are from -120dBm to -80dBm. Then we set the transmit power of our twisted radio wave transmitter so that the received signal strength by the matched receiver is about -100dBm, as shown in Fig. 7. These measurement were taken in order to show the co-existence capability of our twisted radio wave transceiver system with existing Wi-Fi and ZigBee signals.

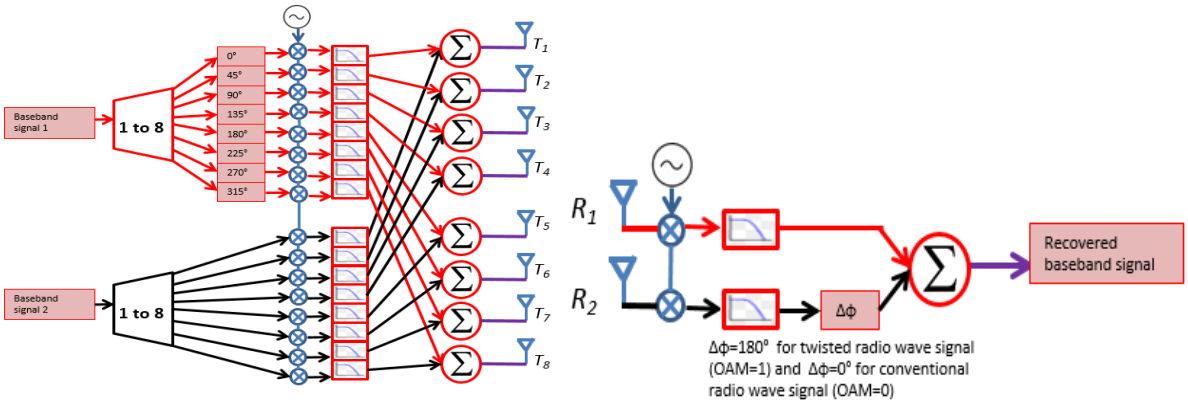

(a) (b)

Figure 6: (a) Block diagram for twisted radio wave transmitter. (b) Block diagram for matched receiver.

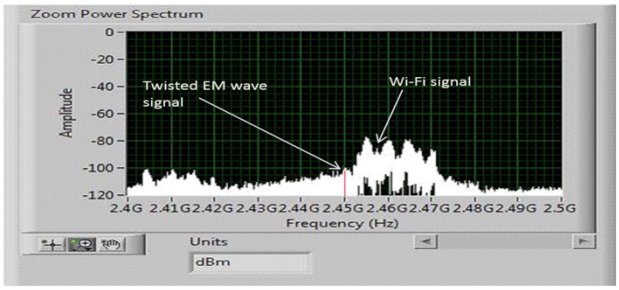

Figure 7: Coexistence of Twisted EM wave signal and Wi-Fi signals in the Project room, INFINITUS.

Fig. 8 shows the actual placement of the transmitter and receiver in the computer room (6.2m x 4.1m) and project room (9m x 5.4m), INFINITUS, school of EEE, NTU. Fig. 9(a) shows the geometry of the computer room, where the transmitter is 3m away from the receiver in LOS condition. Using Ray tracing techniques, all the significant propagation paths including LOS, reflections from walls, floor and ceiling (all assumed to be made of concrete) have been taken in to consideration [23], [24] and modelled according to the properties of concrete [24], i.e. $\epsilon_r = 15$ and $\sigma = 0$. Fig. 9(b) depicts the performance of the simulated path loss profile and makes comparison with the experimental result.

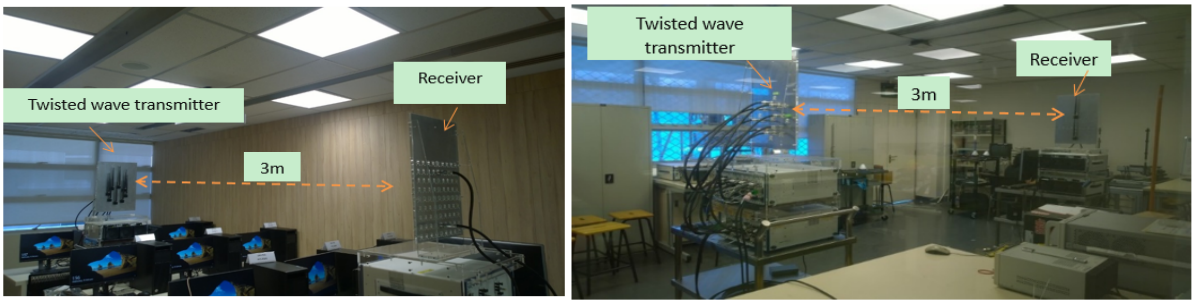

(a) (b)

Figure 8: (a) Twisted radio wave transmitter and receiver placed 3m apart in the computer room, INFINITUS, School of EEE, NTU. (b) Twisted radio wave transmitter and receiver placed 3m apart in the Project room, INFINITUS, School of EEE, NTU.

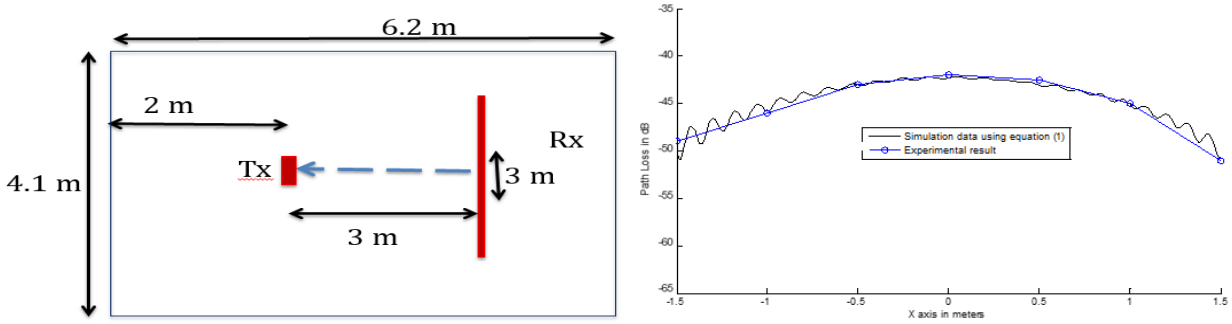

(a) (b)

Figure 9: (a) Geometry for the experiment in computer room, INIFNITUS, when the axis of propagation is parallel to the wall. (b) Comparison of path loss profile for simulation and experiment in the computer room, INFINITUS.

As shown in the Fig. 9(b), the simulated path loss profile reach its peak at the center around -37 dB and fades when moving away where it measured -45dB at 1.5m away. This characteristics also can be observed in the experiment result. It indicates when the transceiver is aligned, the matched receiver is capable of enhancing the LOS twisted radio wave signal while discriminating the reflected signal. This results in a stable transmission link when the twisted radio wave transmitter and receiver are aligned, i.e. at x=0. Our simulations results show that change in ϵ_r from 6 to 15 does not affect the results significantly.

After that, we conducted the experiment in the project room, as shown in Fig. 8(b), which consists of benches, chairs, metal cabinets and electrical measuring equipment such as Oscilloscope, Function generators, power supplies, etc. Fig. 10(a) shows the corresponding geometrical placement, where the transmitter is 3m away from the receiver in LOS condition. Fig. 10(b) shows the performance of the simulated path loss profile and makes comparison with the experimental result. The both experiment and simulation results shows a similar trend to that of Fig. 9(b), which was conducted in the computer room. The results shows the robustness of our system in different propagation environment.

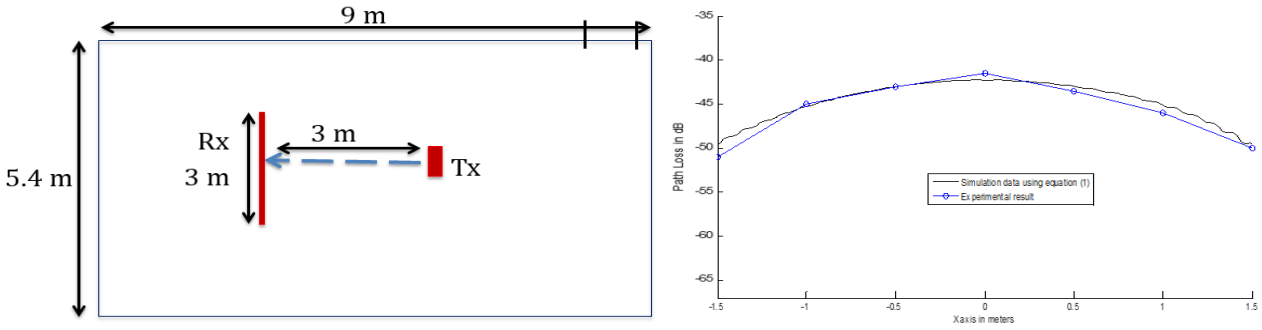

(a) (b)

Figure 10: (a) Geometry for the experiment in the Project room, INIFNITUS, when the axis of propagation is parallel to the wall. (b) Comparison of path loss profile for simulation and experiment, when the axis of propagation is parallel to the wall, in the Project room INFINITUS.

In addition to further test the capabilities of our system in the presence of strong reflections, we placed back the transmitter and receiver along with an Aluminum reflector (2m x 2m) as shown in Fig. 11 and 12(a). The corresponding path loss pattern for simulation and experiment are shown in Fig. 12(b). The results depicts that

our proposed twisted radio wave system shows minimum fluctuations (±2 dB compared to without Aluminum reflector) when the twisted radio wave transceiver is aligned (x=0), even in the presence of Aluminum reflector.

For the final set of experiments, we placed back our twisted radio wave transmitter and receiver according to the geometry shown in Fig. 8(b) and 10(a). The receiver is placed 3m from the transmitter (z=3m), at x=0. Then we simultaneously transmitted 1 kHz twisted radio wave signal modulated with OAM 1and 2 kHz conventional radio wave signal. The path loss pattern was observed over a period of 3 minutes and the corresponding results are shown in Fig. 13, where the path loss component by twisted radio wave signal is shown in red color while that of conventional radio wave is shown in blue color. It could be observed that the path loss component for twisted radio wave shows minimum fluctuations up to ±2dB while that of conventional radio wave signal shows large fluctuations up to ±10dB. These observations further prove that our proposed twisted radio transceiver could provide a very stable link for indoor wireless communication system.

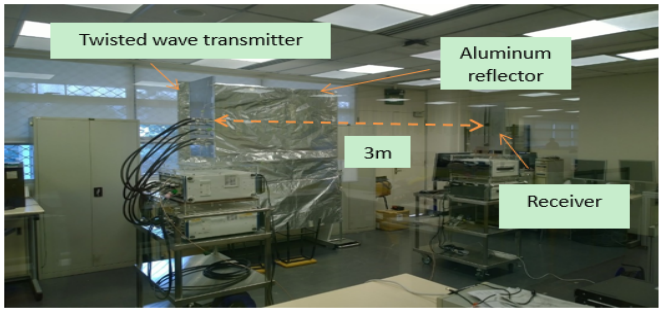

Figure 11: Twisted radio wave transmitter and receiver placed 3m apart in the Project room, INFINITUS, School of EEE, NTU, in the presence of Aluminum reflector.

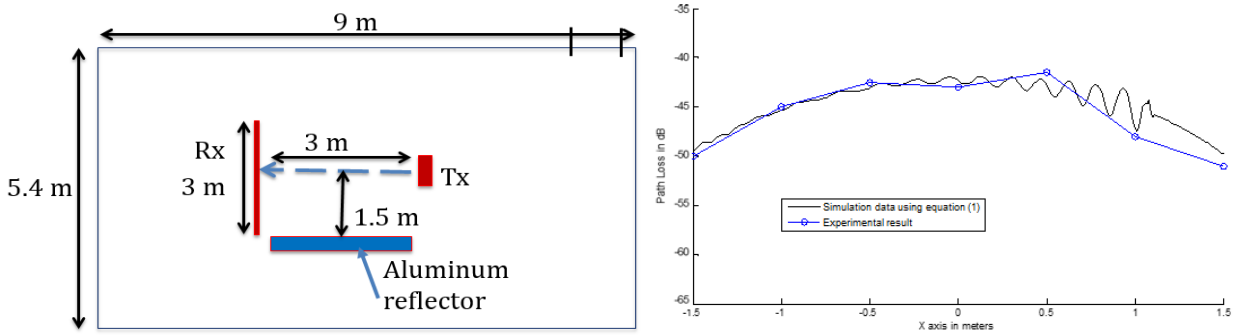

(a) (b)

Figure 12: (a) Geometry for the experiment in the Project room, INIFNITUS Lab, in the presence of Aluminum reflector. (b) Comparison of path loss profile for simulation and experiment in the Project room, INIFNITUS Lab, in the presence of Aluminum reflector.

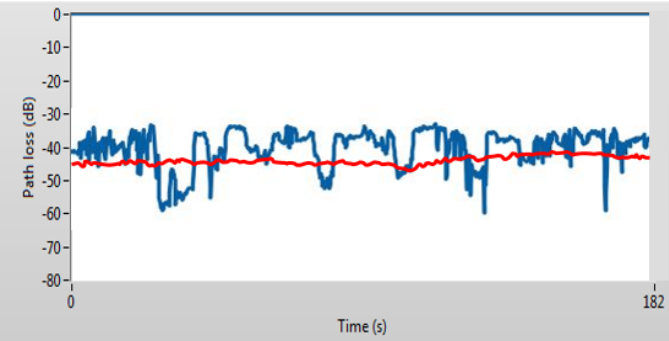

Figure 13: Comparison of path loss component by Twisted Radio wave signal (red) and conventional radio wave signal (blue), over a duration of three minutes in INFINTUS Lab.

CONCLUSION

A novel twisted radio wave based wireless communication has been proposed that can perform well in indoor multipath environments. The corresponding simulations and experiment results show the robustness of our proposed system where it can provide a stable indoor wireless transmission link and also the ability of the transmission link to co-exist with existing RF signals in the same frequency band. Further work will be focused on the evaluation of the proposed system in terms of Digital data transmission, Modulation Error Ratio and Bit Error Rate measurements.

REFERENCES

1. W. Cheng, W. Zhang, H. Jing, S. Gao, H. Zhang, "Orbital angular momentum for wireless communications," *IEEE Wireless Communications*, vol. 26, no. 1, pp. 100-107, Feb 2019.
2. S. M. Lloyd, M. Babiker, G. Thirunavukkarasu, and J. Yuan, “Electron vortices: Beams with orbital angular momentum,” *Rev. Mod. Phys*. 89, 035004, 2017.
3. Y. Ren, L. Li, G. Xie, Y. Yan, Y. Cao, H. Huang, N. Ahmed, Z. Zhao, P. Liao, C. Zhang, G. Caire, A. F. Molisch, M. Tur, and A. E. Willner, “Line-of-sight millimeter-wave communications using orbital angular momentum multiplexing combined with conventional spatial multiplexing,” *IEEE Transactions on Wireless Communications*, vol. 16, no. 5, pp. 3151–3161, May 2017.
4. C. Deng, W. Chen, Z. Zhang, L. Yue, and Z. Feng, “Generation of OAM radio waves using circular vivaldi antenna array,” *Int. J. Antennas Propag*., vol. 2013, pp. 1-7, Apr. 2013
5. M. Barbuto, F. Trotta, F. Bilotti, and A. Toscano, "Circular polarized patch antenna generating orbital angular momentum," *Progress In Electromagnetics Research*, Vol. 148, pp. 23-30, Jun. 2014.
6. M. Lin, Y. Gao, P. Liu, and J. Liu, “Theoretical analyses and design of circular array to generate orbital angular momentum,” *IEEE Transactions on Antennas and Propagation*, vol. 65, no. 7, pp. 3510–3519, July 2017.
7. A. E. Willner, Y. Ren, G. Xie, Y. Yan, L. Li, Z. Zhao, J. Wang, M. Tur, A. F. Molish and S. Ashrafi, “Recent advances in high-capacity free-space optical and radio-frequency communications using orbital angular momentum multiplexing,” *Philos. Trans. Roy. Soc. A, Math., Phys. Eng. Sci*., vol. 375, no. 2087, pp 1-18, Feb. 2017.
8. B. Thide, H. Then, J. Sjoholm, K. Palmer, J. Bergman, T. D. Carozzi, Ya. N. Istomin, N. H. Ibragimov, and R. Khamitova, “Utlilization of photon orbital angular momentum in the low-frequency radio domain,” *Phys.*

Rev. Lett., vol. 99, no. 8, p. 087701, Aug. 2007.

9. F. Tamburini, E. Mari, A. Sponselli, B. Thide, A. Bianchini, and F. Romanato, "Encoding many channels on the same frequency through radio vorticity: first experimental test," *New J. Phys*. Vol. 14, p. 033001, Mar. 2012.
10. K. Liu, Y. Cheng, X. Li, H. Wang, Y. Qin, and Y. Jiang, "Study on the theory and method of vortex-electromagnetic-wave-based radar imaging," *IET Microw. Antennas Propag*. vol. 10, no. 9, pp. 961-968, Jun. 2016.
11. K. Liu, Y. Cheng, Z. Yang, H. Wang, Y. Qin, and X. Li, "Orbital-angular-momentum-based electromagnetic vortex imaging," *IEEE Antennas Wireless Propag. Lett*., vol. 14, pp. 711-714, Mar. 2015.
12. T. Yuan, Y Cheng, H, Wang and Y Qin, "Beam Steering for Electromagnetic Vortex Imaging Using Uniform Circular Arrays", *IEEE Antennas and Wireless Propag. Lett*, vol. 16, pp. 704-707, Aug. 2016.
13. M. Lin, Y. Gao, P. Liu and J. Liu, "Super-resolution orbital angular momentum based radar targets detection", *ELECTRONIC LETTERS*, vol. 52, no. 13, pp. 1168–1170, 23 June. 2016.
14. K. Liu, H. Liu, Y. Qin, Y. Cheng, S. Wang, X. Li, and H. Wang, "Generation of OAM beams using phased array in microwave band," *IEEE Trans. Antennas Propag*., vol. 64, no. 9, pp. 3850-3857, Sep. 2016.
15. Y.Yan, G. Xie, M. P. J. Lavery, H. Huang, N. Ahmed, C. Bao, Y. Ren, Y. Cao, L. Li, Z. Zhao, A. F. Molich, M. Tur, M. J. Padgett, and A. E. Willner, "High-capacity millimetre-wave communications with orbital angular momentum multiplexing," *Nat. Commun*. , vol. 5, p. 4876, Sep 2014.
16. Y. Yan, L. Li, G. Xie, C. Bao, P. Liao, H. Huang, Y. Ren, N. Ahmed, Z. Zhao, Z. Wang, N. Ashrafi, S. Ashrafi, S. Talwar, S. Sajuyigbe, M. Tur, A. F. Molich, and A. E. Willner, "Experimental measurements of Multipath induced intra and inter channel crosstalk effects in millimeter-wave wireless communication using orbital angular momentum multiplexing," *IEEE International Conference on communications (ICC)*, pp. 1370-1375, Sep. 1996.
17. S. W. Chen, C. K. Seow, and S. Y. Tan, "Elliptical Lagrange-Based NLOS Tracking Localization Scheme", *IEEE Trans. Wireless Communications*. vol. 15, no. 5, pp. 3212-3225, May 2016.
18. S. W. Chen, C. K. Seow, and S. Y. Tan, "Virtual Reference Device-Based NLOS Localization in Multipath Environment," *IEEE Antennas and Wireless Propagation Letters*, vol. 13, pp. 1409-1412, Jul. 2014
19. H. Zhang, S. Y. Tan, C. K. Seow, "TOA based Indoor Localization and Tracking with Inaccurate Floor Plan Map via MRMSC-PHD Filter," *IEEE Sensor Journal*, Jul. 2019.
20. H. Zhang, C. K. Seow, and S. Y. Tan, "Virtual reference device-based narrowband TOA localization using LOS and NLOS path," *IEEE/ION Position, Location and Navigation Symposium (PLANS)*, pp. 225–231, April 2016.
21. S. W. Chen, C. K. Seow, and S. Y. Tan, "Single reference mobile localisation in multipath environment," *Electronics Letters*, vol. 49, no. 21, pp. 1360–1362, Oct. 2013.
22. Constantine A. Balanis, "Linear Wire Antennas", *Antenna Theory Analysis and Design*, 3rd ed, John Wiley & Sons, Inc., New Jersey, USA
23. S. Y. Tan and H. S. Tan, "A Microcellular Communications Propagation Model Based on the Uniform Theory of Diffraction and Multiple Image Theory", *IEEE Trans. Antennas and Propag*. vol. 44, no. 10, pp. 1317-1326, Oct. 1996.
24. S. Y. Tan and H. S. Tan, "Improved three-dimensional ray tracing technique for microcellular propagation models", *Electronics Letters*., vol. 31, no. 17, pp. 1503-1505, Aug. 1995.